REST Journal on Emerging trends in Modelling and Manufacturing
Vol:2(4),2016
REST Publisher
ISSN: 2455-4537

Website: www.restpublisher.com/journals/jemm

Effect of bend curvature on velocity & pressure distribution from straight to a 90° pipe bend - A Numerical Study

Prasun Dutta[1*] and Nityananda Nandi[2]

[1,2]Department of Aerospace Engineering and Applied Mechanics, Indian Institute of Engineering Science and Technology, Shibpur, West Bengal, India – 711103

[1*]pd.iiest@gmail.com, [2]nityananda@mailcity.com

ABSTRACT

The present work deals with the numerical study of single-phase turbulent flow through a 90° pipe bend using *k-ε* turbulence model. A detailed study has been carried out to investigate the effect of bend curvature on both axial velocity and static pressure distribution at different sections inside of pipe bend as well as adjacent sections of bend inlet (upstream) and outlet (downstream). Contour plots of both normalized axial velocity, static pressure as well as axial velocity profiles at different section are presented in graphical form. The effect of bend curvature on velocity and static pressure is clearly observed and discussed here.

Key Words: *k–ε* turbulence model, Pipe bend, Turbulent Flow, Pressure and Velocity distribution.

INTRODUCTION

Different types of fluid flow, such as air, water, oil, etc. through pipe bends has been of considerable interest to the many engineering applications. Investigations of the flow through bends are of great significance in understanding and improving their performance and minimizing the losses. It is already well known that the flow of incompressible viscous fluids through pipe bends are characterized by flow separation, secondary flow, and unsteadiness which are dependent on Reynolds number as well as the radius of curvature of the bend. The main feature of flow through a bend is the presence of a radial pressure gradient created by the centrifugal force acting on the fluid. Because of this, the fluid at the centre of the pipe moves towards the outer side and comes back along the wall towards the inner side. If the bend curvature is strong enough, the adverse pressure gradient near the outer wall in the bend and the inner wall just after the bend may lead to flow separation at these points, giving rise to a substantial increase in pressure losses. The pressure losses suffered in a bend are caused by both friction and momentum exchanges resulting from a change in the direction of flow. Both these factors depend on the bend angle, the curvature ratio and the Reynolds Number. Therefore, investigations of the flow through bends are of great significance in understanding and improving their performance and minimizing the losses. Recently the use of pipe bends played a major role in the nuclear reactor cooling system; this has also attracted the interest of the researchers (Ono 2011, Takamura 2012, Dutta et al. 2016, Dutta and Nandi 2015a). Very recent study on turbulent characteristics for single phase flow in large bends provides a new mathematical model for predicting pressure loss (Liwei et al., 2012), and a detailed study on characteristics of secondary flow and decay of swirl intensity on pipe bends (Kim et al., 2014). Many experimental studies have been conducted to date to clarify the flow and pressure fields in the pipe bend flows. Frequency characteristics of pressure fluctuation and the total pressure loss coefficient were studied at very high Re, over 10^6 by Shiraishi et al. 2006, 2009. In these studies, it was shown that a power spectrum density (PSD) profile of pressure fluctuation obtained near the flow separation region had a peak at Strouhal number (St = 0.5) based on the mean axial velocity and pipe diameter, and this characteristic of pressure fluctuation was shown in the wide range of Reynolds number (Yamano et al. 2009). According to Takamura et al. 2012, Ebara et al. 2016, the flow structure in the single elbow piping can be inferred to have three periodic motions, i.e., periodic vortices shedding in the shear flow region between the flow separation region and high-velocity region near the pipe centre, periodic separated vortices shed from the separation region, and periodic circumferential flows toward the intrados side. On the subject of the pressure fluctuation characteristic, is found normalized PSD profiles were independent of Reynolds number, and showed good agreement with each other (Ebara et al. 2010). However, some researchers have already made a significant contribution on the subject; much is yet to be done to present a clear picture of the fundamental characteristics of pressure and velocity distribution.

GOVERNING EQUATIONS AND NUMERICAL METHODOLOGY

In the present study Reynolds Averaged Navier-Stokes (RANS) equations are solved using the segregated implicit solver. The second order scheme is utilized for the RANS equations calculations, with a pressure-velocity coupling achieved using SIMPLE algorithm. The default under relaxation factors was used to aid convergence for all models.

The governing equations for incompressible fluid flow with constant properties are

$$\frac{\partial u_i}{\partial x_i} = 0 \tag{1}$$

$$\frac{\partial u_i}{\partial t} + u_j \frac{\partial u_i}{\partial x_j} = f_i - \frac{1}{\rho}\frac{\partial p}{\partial x_i} + \upsilon \frac{\partial^2 u_i}{\partial x_j \partial x_j} \tag{2}$$

Equations (1) and (2) are conservation of mass and momentum, respectively, fi is a vector representing external forces, υ is the kinematic viscosity. The k-ε turbulence model is adopted for the present study as k-ε turbulence model performs better for single-phase flows in pipe bend (Kim et al. 2014, Homicz 2004, Dutta and Nandi. 2015b, Dutta et al. 2015c). The turbulence kinetic energy (k) and the turbulence dissipation rate (ε) are solved to determine the coefficient of turbulent viscosity (μt).

$$\frac{\partial(pk)}{\partial t} + \frac{\partial(pku_i)}{\partial x_i} = \frac{\partial}{\partial x_j}\left[\frac{\mu_t}{\sigma_k}\frac{\partial k}{\partial x_j}\right] + 2\mu_t E_{ij} E_{ij} - \rho\varepsilon \tag{3}$$

$$\frac{\partial(p\varepsilon)}{\partial t} + \frac{\partial(p\varepsilon u_i)}{\partial x_i} = \frac{\partial}{\partial x_j}\left[\frac{\mu_t}{\sigma_\varepsilon}\frac{\partial k}{\partial x_j}\right] + C_{1\varepsilon}\frac{\varepsilon}{k}2\mu_t E_{ij}E_{ij} - C_{2\varepsilon}\rho\frac{\varepsilon^2}{k} \tag{4}$$

Where; u_i represents velocity component in the corresponding direction, E_{ij} represents a component of the rate of deformation, μt represents eddy viscosity. The equations (3) and (4) also consist of some adjustable constants (Tu et al. 2012), these are as follows

$$C_\mu = 0.09, \sigma_\kappa = 1.00, \sigma_\varepsilon = 1.30, C_{1\varepsilon} = 1.44, C_{2\varepsilon} = 1.92$$

The second order upwind scheme is used for the present calculations, with a pressure-velocity coupling achieved using SIMPLE algorithm. The default under relaxation factors was used to aid convergence for the model.

PROBLEM DEFINITION AND BOUNDARY CONDITIONS

The present work is a numerical study, utilizing k-ε turbulence model to explore the effect of curvature on the velocity distribution at different sections of pipe bend. The problem that is considered here is the fluid flow through 90° pipe bends having an inner diameter of 0.01 m with curvature ratio (Rc/D) = 2 for Reynolds number 1×10^5. The inlet length of straight pipe in the calculations was set up 20D to save computational time. The three-dimensional structured mesh was used containing hexahedron elements, which was optimized via a grid independence study. The bend geometry and mesh are shown in Figure 1(a) and (b) respectively. It is defined that the axial direction downstream the bend is x-coordinate, the direction from the inner core to outer core of the bend is y-coordinate, and the perpendicular direction to x and y is z-coordinate. Three types of boundary conditions have been specified for the computational domain. At the inlet, the measured inlet velocity (U_{in}), the turbulence intensity ($I= 0.16\times Re^{-0.125}$), hydraulic diameter = 0.01m are given. At the wall boundaries, the no-slip conditions have been applied, and at the outlet, outflow boundary conditions have been implemented.

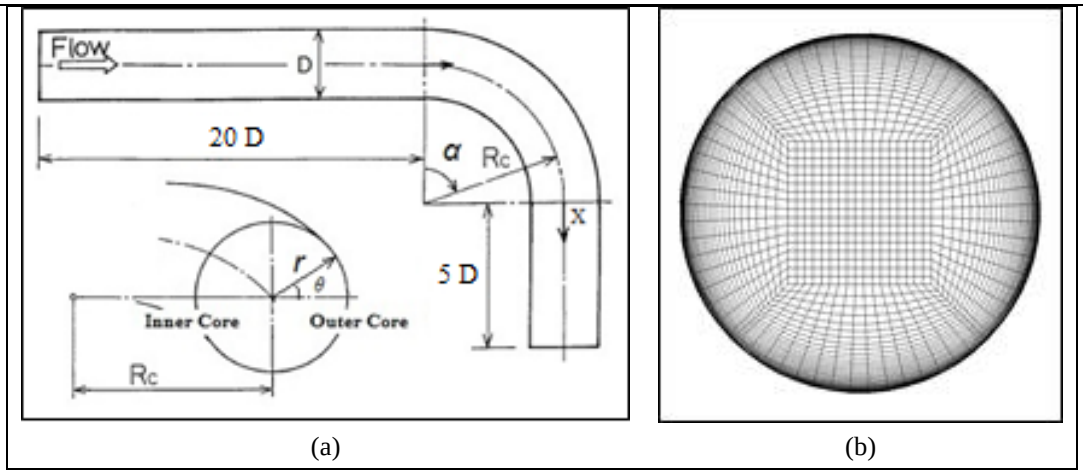

Figure 1: Schematic diagram of the (a) bend geometry and (b) present model with the computational grid.

Before starting of the present study, our model and simulation setup are first validated against the existing experimental and numerical data by (Tanaka et al. 2009, Sudo et al. 1998, Kim et al. 2014). The mean axial velocity profile normalized with inlet velocity along symmetry line at bend outlet (α = 90°) show excellent agreement with both experimental and numerical results (Figure 2). From the validation part, it has been seen that model is in close approximation with the published results. Hence this procedure of mesh generation and simulation setup has been used for further analysis.

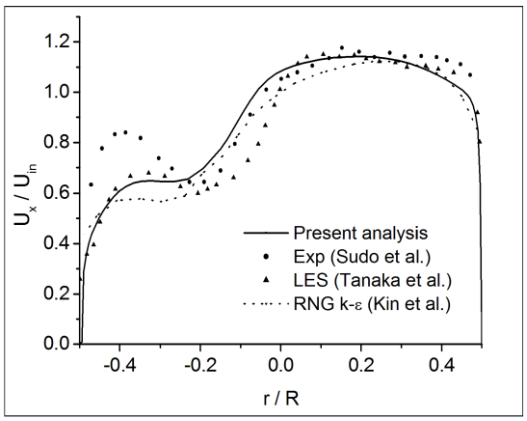

Figure 2: Comparison of the normalized axial velocity profile of present analysis with published experimental and numerical results.

RESULTS AND DISCUSSIONS

The main objective of the present study is to explore the effect of curvature on the velocity and static pressure distribution from straight to curved zone in a 90° pipe bend through numerical simulation. The results of the normalized axial velocity profile, contour plots of normalized axial velocity and static pressure at different positions (upstream, inside pipe bend and downstream) are presented in this section.

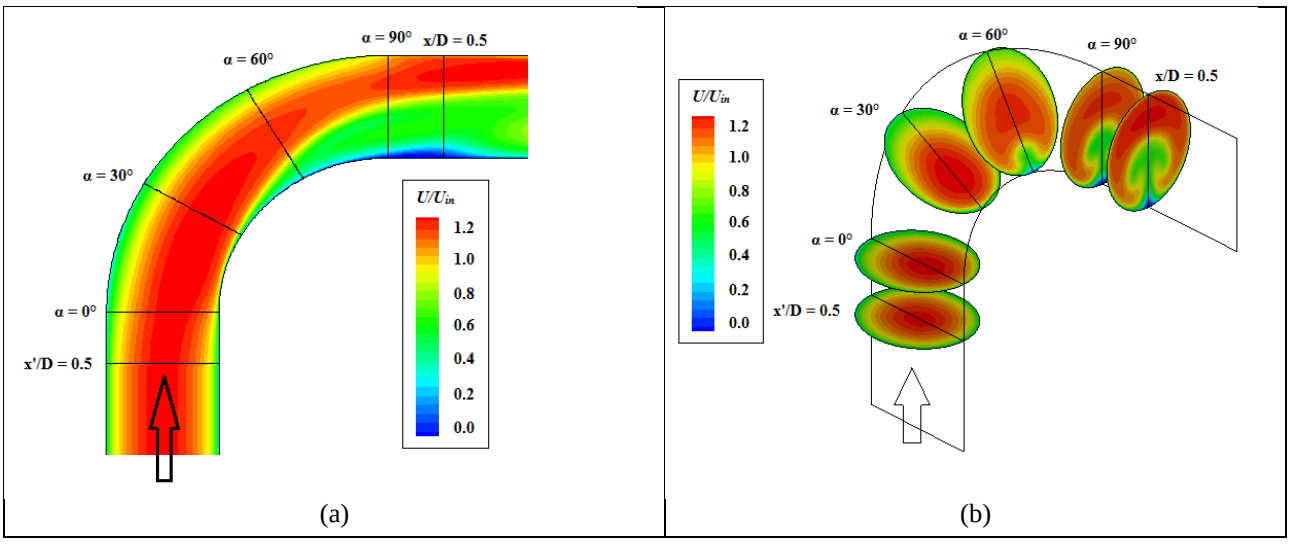

Figure 3: Contour plot of the axial velocity (U) normalized with inlet velocity (Uin) at different sections of the pipe bend. (a) Symmetry plane, (b) Different sections as indicated in figures.

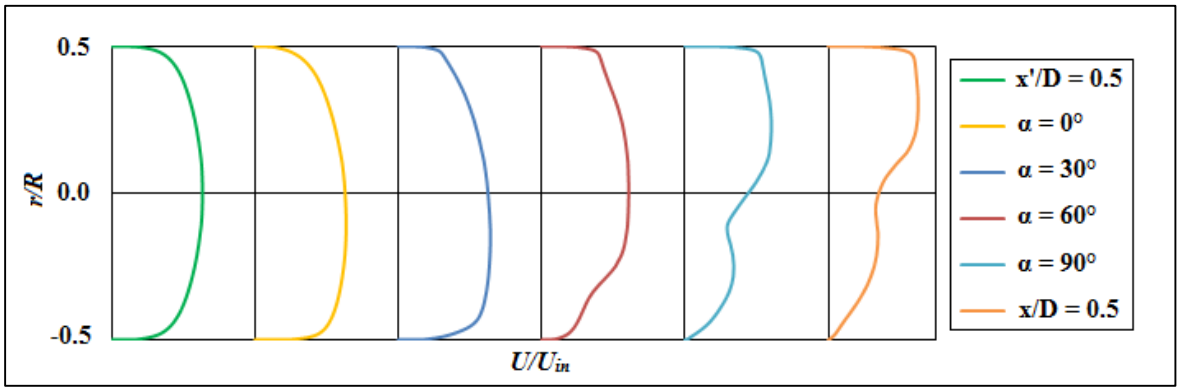

Figure 4: Normalized velocity profiles at different positions throughout the bend.

The effect of curvature can be clearly seen in Figure 3. At the upstream section (x'/D = 0.5) the velocity profile shows that it is magnitude is maximum at the middle portion of the pipe. When it moves inside the bend, this maximum velocity tends to occur towards the outer wall of the bend gradually and near the outlet section (α = 90°) this maximum velocity occurs fully at the outer wall. A low-velocity region is also observed near the inner wall beyond the bend outlet (α = 90°). Figure 4 shows normalized axial velocity profiles at different positions in symmetry plane as indicated in figure 4.The negative value of y–axis indicates the inner wall of the bend. Velocity profiles are found irregular throughout the pipe bend and both magnitude and nature change as flow moves through the pipe bend due to the effect of the curvature of pipe bend. The nature of the velocity profiles of both upstream section (x'/D = 0.5) and the bend inlet (α = 0°), are more or less same. The velocity gradient at the outer wall of the inlet section is greater than the velocity gradient of the section upstream of the inlet that is in the straight zone. The velocity magnitude at the inner wall of the inlet section is greater that the velocity magnitude of the section upstream of the inlet that is in the straight zone. Similarly, the velocity magnitude of the outer wall at the section downstream to the bend outlet is greater than the velocity magnitude at the outer wall of bend outlet section, and at the inner wall of bend outlet section, velocity magnitude is higher than that of the section downstream to the bend outlet which is in the straight portion. At the outer wall, the velocity gradient of outlet section is higher than that of the section downstream to the bend outlet that is in the straight portion. Velocity profiles are found different at the upstream and downstream section due to the effect of curvature, although they are straight sections.

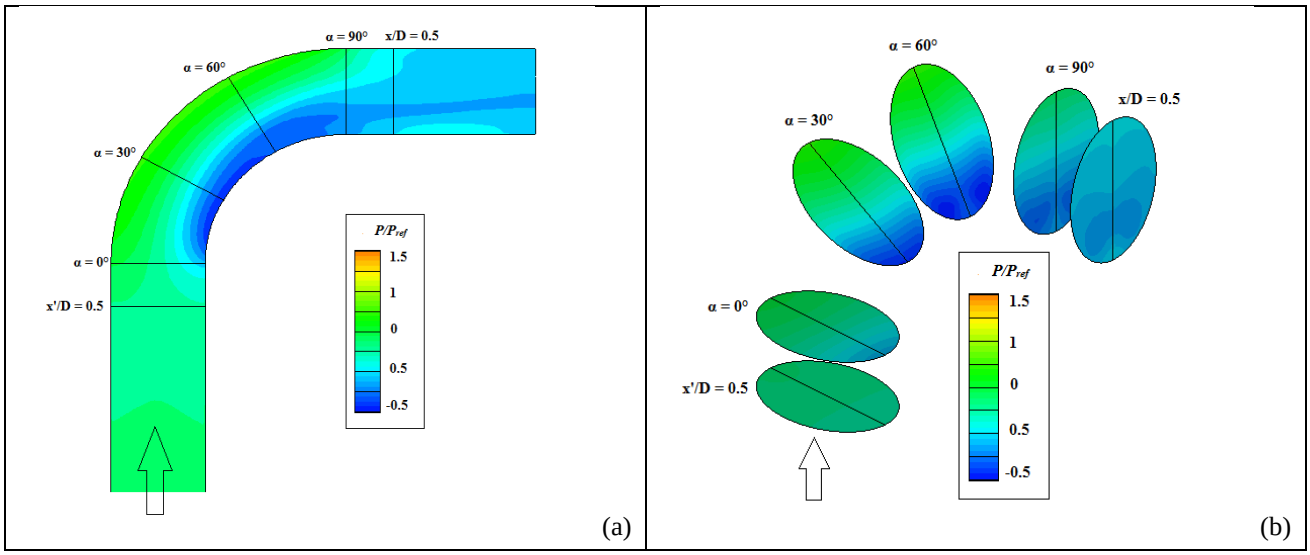

Figure 5: Contour plot of the normalized static pressure (P/P_{ref}) at different sections of the pipe bend. (a) Symmetry plane, (b) Different sections as indicated in figures.

Figure 5 shows the contour plots of static pressure normalized with reference pressure taken at x'/D = -17.6 as suggested by Sudo et al. 1998) at different sections of the pipe bend. (a) Symmetry plane, (b) Different sections as indicated in the figure. The effect of curvature can be clearly seen in Figure 3. At the upstream straight section (x'/D = 0.5) adjacent to the bend inlet (α = 0°) which is in the straight portion of the pipe, the normalized pressure is found a uniform. As flow enters to the bend inlet, the pressure increases on the outer while the pressure on the inner wall experiences a gradual drop. This change in normalized pressure from the uniform value of static pressure before the bend inlet that is in straight section is caused due to the curvature of the bend. As flow moves through the pipe bend from bend inlet (α = 0°) to bend outlet (α = 90°), the pressure on the outer wall experiences a rapid growth whereas the pressure on the inner wall experiences a sharp drop under the impact of the centrifugal force resulting from the circular motion of fluid particles induced by curvature of the pipe bend. Between α = 30° to α = 60° sections inside the bend, the high-pressure zone is found in the outer wall of the bend, and a low-pressure zone is located in the inner wall of the bend. As flow approaches to the vicinity of the α = 50∘ cross section of pipe bend, pressure on the outer wall reaches its maximum value while pressure on the inner wall attains its minimum value. On the outer wall, this is caused by both of the centrifugal forces and the impact of the fluid on the elbow wall due to the effect of the curvature of the bend. On the inner wall, the decline and the minimum of the pressure is induced partially by the boundary-layer separation. After this region, the pressure of the outer wall begins to decrease due to the reflection effect of the fluid particle from outer wall to the inner wall. As the fluid leaves the bend, the flow now has become highly complicated and it tries to stabilize itself. At the outer wall of the adjacent section (x/D = 0.5) to the bend outlet that is in the straight portion of the downstream pipe, normalized pressure is found less than the normalized pressure at the outer wall of bend outlet. Similarly, at the inner wall of x/D = 0.5 section, the normalized pressure is found more than the normalized pressure at the inner wall of bend outlet.

CONCLUSIONS

The following findings can be made from the present study:

- As soon as the flow enters the bend, the velocity profile becomes irregular, and when it moves inside the bend, the maximum velocity tends to occur towards the outer wall of the bend gradually. Near the outlet section, this maximum velocity occurs fully at the outer wall which is due to the effect of curvature.
- At bend inlet and a section upstream to the bend inlet which is in the straight part of the pipe, the nature of velocity profiles is more or less same. However the velocity gradient at the outer wall of the straight portion is greater than that of bend inlet section, and at the inner wall, velocity magnitude of inlet section is higher than that of the section upstream to the bend inlet.
- The velocity magnitude of the outer wall at the section downstream to the bend outlet is greater than that of the section of bend outlet section, and at the inner wall, velocity magnitude of outlet section is larger than that of the section downstream to the bend outlet that is in the straight zone.
- At the upstream straight section adjacent to the bend inlet which is in the straight portion of the pipe, the normalized pressure is found a uniform. As flow enters to the bend inlet, the pressure increases on the outer while the pressure on the inner wall experiences a gradual drop.
- Inside the pipe bend, the high-pressure region is found at the outer wall, and a low-pressure zone is located at the inner wall. Normalized pressure is found maximum at the outer wall near the vicinity of α = 50° of the bend section and minimum at the inner wall of the same bend section.
- After the bend outlet, flow tries to stabilize itself and normalized pressure decreases at the outer wall whereas normalized pressure increases at the inner wall. Normalized pressure is found less at the outer wall and more at the inner wall of the adjacent section to the bend outlet which is in the straight portion than the bend outlet section.

ACKNOWLEDGMENTS: This paper is a revised and expanded version of two articles which are presented in "Engineering Problems and Application of Mathematics-2016, NIT Agartala" and "Proceedings of 61st Congress of ISTAM - 2016, VITU - Vellore, India".

REFERENCES

[1]. Dutta, P., & Nandi, N. (2015a). Effect of Reynolds Number and Curvature Ratio on Single Phase Turbulent Flow in Pipe Bends. *Mechanics and Mechanical Engineering*, *19*(1), 5-16.

[2]. Dutta, P., Saha, S. K., & Nandi, N. (2015b). Computational study of turbulent flow in pipe bends. *International Journal of Applied Engineering Research*, 10(11), 1028-1033.

[3]. Dutta, P., & Nandi, N. (2015c). Study on pressure drop characteristics of single-phase turbulent flow in pipe bend for high Reynolds number. *ARPN J. Eng. Appl. Sci*, 10(5), 2221-2226.

[4]. Dutta, P., Saha, S. K., Nandi, N., & Pal, N. (2016). Numerical study on flow separation in 90° pipe bend under high Reynolds number by k-ε modeling. *Engineering Science and Technology, an International Journal*, *19*(2), 904-910.

[5]. Ebara, S., Aoya, Y., Sato, T., Hashizume, H., Kazuhisa, Y., Aizawa, K., & Yamano, H. (2010). Pressure Fluctuation Characteristics of Complex Turbulent Flow in a Single Elbow With Small Curvature Radius for a Sodium-Cooled Fast Reactor. *Journal of Fluids Engineering*, *132*(11), 111102.

[6]. Ebara, S., Takamura, H., Hashizume, H., & Yamano, H. (2016). Characteristics of flow field and pressure fluctuation in complex turbulent flow in the third elbow of a triple elbow piping with small curvature radius in three-dimensional layout. *International Journal of Hydrogen Energy*, *41*(17), 7139-7145.

[7]. Homicz, G. F. (2004). Computational fluid dynamic simulations of pipe elbow flow. United States. Department of Energy.

[8]. Kim, J., Yadav, M., & Kim, S. (2014). Characteristics of Secondary Flow Induced by 90-Degree Elbow in Turbulent Pipe Flow. *Engineering Applications of Computational Fluid Mechanics*, *8*(2), 229-239.

[9]. Ono, A., Kimura, N., Kamide, H., & Tobita, A. (2011). Influence of elbow curvature on flow structure at elbow outlet under high Reynolds number condition. *Nuclear Engineering and Design*, *241*(11), 4409-4419.

[10]. Shiraishi, T., Watakabe, H., Sago, H., Konomura, M., Yamaguchi, A., & Fujii, T. (2006). Resistance and fluctuating pressures of a large elbow in high Reynolds numbers. *Journal of fluids engineering*, *128*(5), 1063-1073.

[11]. Shiraishi, T., Watakabe, H., Sago, H., & Yamano, H. (2009). Pressure fluctuation characteristics of the short-radius elbow pipe for FBR in the postcritical Reynolds regime. *Journal of Fluid Science and Technology*, *4*(2), 430-441.

[12]. Sudo, K., Sumida, M., & Hibara, H. (1998). Experimental investigation on turbulent flow in a circular-sectioned 90-degree bend. *Experiments in Fluids*,*25*(1), 42-49.

[13]. Takamura, H., Ebara, S., Hashizume, H., Aizawa, K., & Yamano, H. (2012). Flow visualization and frequency characteristics of velocity fluctuations of complex turbulent flow in a short elbow piping under high Reynolds number condition. *Journal of Fluids Engineering*, *134*(10), 101201.

[14]. Tanaka, M. A., Ohshima, H., & Monji, H. (2009, January). Numerical Investigation of flow structure in pipe elbow with large eddy simulation approach. In *ASME 2009 Pressure Vessels and Piping Conference* (pp. 449-458). American Society of Mechanical Engineers.

[15]. Tu, J., Yeoh, G. H., & Liu, C. (2012). *Computational fluid dynamics: a practical approach*. Butterworth-Heinemann.

[16]. Wang, L., Gao, D., & Zhang, Y. (2012). Numerical simulation of turbulent flow of hydraulic oil through 90° circular-sectional bend. *Chinese Journal of Mechanical Engineering*, *25*(5), 905-910.

[17]. Yamano, H., Tanaka, M., Kimura, N., Ohshima, H., Kamide, H., & Watanabe, O. (2009). Unsteady hydraulic characteristics in large-diameter pipings with elbow for JSFR.(1) Current status of flow-induced vibration evaluation methodology development for the JSFR pipings.